2018

Analog Temperature Control Circuit for a Thin-Film Piezoelectric-on-Substrate Microelectromechanical Systems Oscillator

Heather Hofstee
University of Central Florida

ANALOG TEMPERATURE CONTROL CIRCUIT FOR A THIN-FILM PIEZOELECTRIC-ON-SUBSTRATE MICROELECTROMECHANICAL SYSTEMS OSCILLATOR

by

HEATHER HOFSTEE

A thesis submitted in partial fulfillment of the requirements
for the Honors in the Major Program in Electrical Engineering
in the College of Engineering and Computer Science
and in the Burnett Honors College
at the University of Central Florida
Orlando, Florida

Fall Term, 2018

Thesis Chair: Dr. Reza Abdolvand

ABSTRACT

The objective and motivation for this project is to design a low-power, low-noise oven-control circuit to optimize the stability of a MEMS oscillator. MEMS oscillators can be fabricated using conventional semiconductor manufacturing methods and can often be assembled in packages smaller than those of traditional crystal oscillators. However, one of their largest disadvantages currently is their high temperature coefficient of frequency (TCF), causing MEMS oscillators to be especially sensitive to temperature changes. Hence, this project focuses on designing a printed circuit board that will allow the user to manually tune a current passing through a resonator wire-bonded to the board to elevate the resonator temperature. This will ensure that the device's resonance frequency stays largely constant and that the oscillator provides a very stable signal.

ACKNOWLEDGMENTS

This work would not have been possible without many people along the way. First and foremost, I would like to thank Dr. Reza Abdolvand, my thesis chair, for guiding me and encouraging me and allowing me this opportunity. This has been the most challenging and yet rewarding experience of my collegiate years. Thank you for being the kind of mentor that would give up your lab key so that I could come in early, for teaching me the importance of asking, "Why?", and for the many hours you spent discussing project details.

I would also like to thank the other members of the Dynamic Microsystems Lab group. Thank you all for taking time out of your busy schedules to help me out, for laughing with me, and for making this such a fun experience.

I also owe a debt of gratitude to my family. Their unwavering support has been a stronghold for me, and I am grateful for their understanding and sacrifices for me.

Last but not least, I would like to thank my dear friends at UCF. Thank you for being there for me and for reassuring me when I was overwhelmed. Thank you for encouraging me to follow my dreams and for being so understanding throughout this process. Your support has meant more than you know.

TABLE OF CONTENTS

LIST OF FIGURES

LIST OF TABLES

CHAPTER 1: INTRODUCTION AND OBJECTIVE

1.1 Introduction and Overview

Microelectromechanical systems (MEMS) is an area of research in which much discovery and advancement has been made in the past six decades. MEMS are now used in countless applications, the variety of which is steadily increasing. One of these uses is for circuit timing. Crystal oscillators have long been the device of choice for this application because of their high quality factor and temperature stability; however, MEMS resonators have shown promise for being smaller and having CMOS compatible fabrication processes [1].

MEMS resonators are fabricated on variety of mediums. However, this research will focus on those on a silicon substrate. Silicon has several properties, such as single crystal structure, low motional impedance, and high Q factor, that make it a viable option as a substrate [2].

However, a disadvantage of this substrate is that it tends to have a relatively high temperature coefficient of frequency (TCF) [3]. The TCF of a material such as silicon is dependent on doping and other characteristics of the substrate. This high sensitivity to temperature causes undesirable variations in the resonance frequency. Thus, a method of stabilizing the resonance frequency is sought; an effective method is some form of oven-control. This work explores active temperature compensation as a method of oven-control.

1.2 Objective and Motivation

The objective of this work is to design and build a circuit that will allow for the user to manually stabilize the temperature of a silicon-based MEMS resonator wire-bonded to pads of the PCB at an elevated set point. Because of the characteristic TCF of a TPoS resonator, it is predicted

that parts per billion (ppb) frequency stability is achievable through such temperature stabilization. The purpose of this circuit is to explore the frequency stability of a TPoS MEMS oscillator at a stable temperature equal to the resonator's turn-over temperature (the temperature at which the derivative of the TCF is equal to zero).

A functional block diagram is shown below for an overview of how the circuit operates:

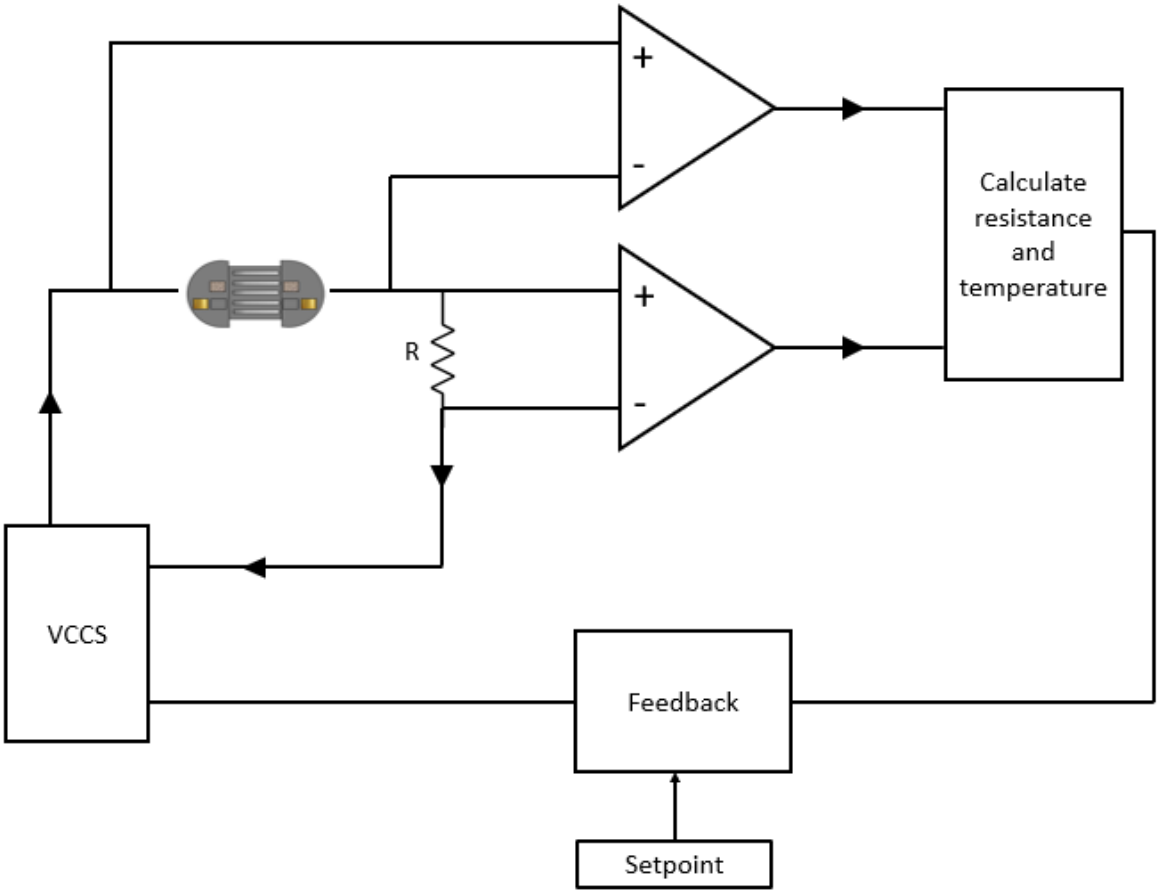

Figure 1: Circuit block diagram

This circuit will use Ohmic resistive heating (also known as Joule heating) to elevate the temperature of the resonator. The principle of this type of heating is that electric current is used to produce heat. Because the resonator is made of doped silicon, passing a current through the

resonator will produce heat in the device. The amount of current needed to heat the resonator above the industrial operating range will be crucial for this project and must be obtained via testing data.

The resistance of the resonator will also change with its temperature. Because the resonator was fabricated on silicon, which is a semiconductor material, the temperature coefficient of resistance will most likely be negative, indicating an inverse relationship between the temperature and the resistance of the resonator. Testing will be done to correlate a particular temperature and resistance of the resonator, and this information will be used to help calculate the temperature of the resonator for any arbitrary current.

The controlled current will also be passed through a resistor with a very low temperature coefficient of resistance (TCR), which guarantees that the resistance of this resistor does not change much over a certain range of temperature. The voltage across this resistor will be measured using an instrumentation amplifier. Knowing the resistance and the voltage across it allows for the current through the resistor to be calculated. Since this resistor is in series with the resonator, the current through the two components will be equal.

Using an instrumentation amplifier, the voltage across the resonator will also be measured. Since the current through the resonator can be calculated using the voltage across a low TCR resistor, the data needed to calculate the resistance of the resonator can be obtained. Then, the resistance of the resonator can be correlated using prior testing data. Each resistance value of the resonator will correspond to a particular temperature, and using this information, the resistance of the resonator can be used to determine the temperature.

Then, the circuit feedback will have to be tuned to set the temperature equal to the set point (which is the turnover temperature of the resonator). The current through the resonator will be controlled using a voltage controlled current source with the voltage manually controlled using a potentiometer. If a certain temperature value is desired, then the voltage input will have to be altered. Through calculation of the resonator resistance and temperature, the user can decide how to adjust the input voltage and thus the resonator current. This feedback loop could eventually be closed using a microcontroller.

CHAPTER 2: BACKGROUND AND MOTIVATION

2.1 Background

Ovenization of MEMs resonator and oscillators is among the most effective active temperature control methods. The idea is to operate the oscillator at a constant elevated temperature to prevent fluctuation. This proposal details a design for an oven-control circuit for a thin-film piezoelectric-on-silicon (TPoS) MEMS resonator. The design will focus on using voltage and current measurements and manual control to keep the temperature of the oscillator above 85°C. The current will also be passed through a filter so that the signal that reaches the resonator will be low noise.

2.2 MEMS Development

A Bell Labs researcher first created “air-isolated integrated circuits” in 1965 [4]. This laid the groundwork for MEMS research and development. In the 1970s, micro sensors and actuators were studied more extensively. Around this time, integrated circuit fabrication technology began to be applied to MEMS technology, specifically bulk micromachining (the usage of chemical etchants to selectively remove silicon to form different microstructures.)

In the 1980s, surface micromachining (where low pressure chemical vapor deposition is used to deposit layers on a substrate and then a sacrificial layer between the substrate and layers is removed) was applied to MEMS fabrication. IBM researchers developed a MEMS accelerometer, and then a vapor sensor was developed at University of California Berkeley (UC Berkeley) using surface micromachining. This opened a new host of possibilities for MEMS.

Micro gears and micro motors were fabricated successfully, introducing potential for resonators and actuators. Researchers at UC Berkeley then developed a polysilicon resonator with electrostatic comb drive structures [4]. The next large focus became packaging, mainly to reduce resonator errors. However, other applications continued to expand as MEMS technology was used for neural interfacing, micro fluids, and other applications.

2.3 Applications and Potential

Currently, piezoelectric devices have a wide variety of applications from transducers and mechanical actuation to microstructure sensing. Microelectromechanical systems (MEMS) have a large potential for new applications. Their ability to be manipulated by electric fields and their small size are very promising because they can easily be integrated into electronic devices [5].

Although research on MEMS is still a developing field, they are prevalent in a number of modern applications. A Texas Instruments employee invented the digital micrometer devices (DMD) for usage in digital displays starting in the 1990s, while UC Berkeley researchers created RF MEMS for wireless communications applications. Bio-MEMS, for usage with biological and chemical devices and often used to deliver nanoliter drops of fluids, were first created in the 1990s as well.

In the 2000s, MEMS started being used as inertial sensors and gyroscopes with the advent of more sophisticated machining techniques [4]. Today, there are a number of other MEMS applications, including inkjet printers, DNA manipulation, scanning probe microscopes, optical fiber switches, and more [6]. This research will focus on MEMS resonators as a replacement for crystal oscillators.

2.4 Crystal Oscillators

Highly prevalent in circuits and integrated circuits (ICs), crystal oscillators are considered to be stable and have a high Q factor [7].

The current larger size of crystal oscillators is more common because they are less expensive than smaller applications. However, smaller crystal oscillators are increasingly in higher demand because of the decrease in overall size of electronics.

Crystal oscillators do have some disadvantages compared to MEMS resonators. For some applications, MEMS resonators may be a more suitable choice because they are often smaller in size and can usually be fabricated directly on an IC.

2.5 Piezoelectricity

Piezoelectricity was first discovered by the Curie brothers. However, it was not until 1921 that the piezoelectric properties of quartz allowed crystal resonators to be used as oscillators [5]. Currently, some common piezoelectric materials are aluminum nitride (AlN), lithium niobate ($LiNbO_3$), quartz, lead zirconate titanate (PZT), and zinc oxide (ZnO) [8].

Largely dependent on crystal orientation, the direct piezoelectric effect occurs when charge is generated from external stress or strain. This external force alters the spacing between the positive and negative charges, causing a measurable open circuit voltage on the crystal surface [8].

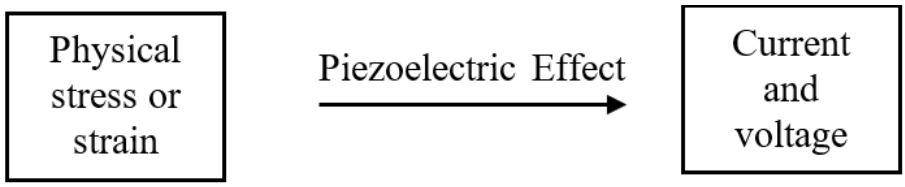

Figure 2.1: Piezoelectric effect

Mathematically, the piezoelectric effect can be described by the following formula:

$$D = dT + \varepsilon E \qquad (2.1)$$

where D is the electrical polarization, d is the piezoelectric coefficient matrix, T is the applied mechanical stress, ε is the electrical permittivity matrix, and E is the electric field strength.

Through the inverse piezoelectric effect, a mechanical force can be caused by the application of an electric field. This creates a force between the positive and negative charges and causes elastic strain and stress.

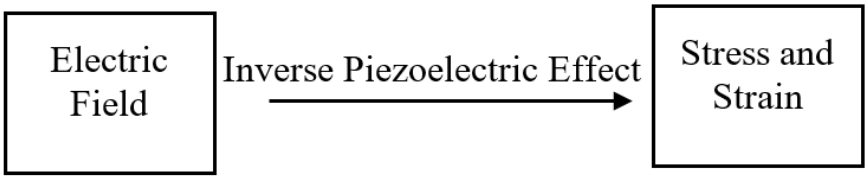

Figure 2.2: Inverse piezoelectric effect

Mathematically, the inverse piezoelectric effect can be described by the following formula:

$$s = ST + dE \quad (2.2)$$

where s is the strain vector, S is the compliance matrix, T is the applied mechanical stress, d is the piezoelectric coefficient matrix, and E is the electrical field strength.

2.6 Fundamentals of Resonators

A resonator is a device that exhibits resonance, such that it oscillates mechanically with greater amplitude at certain frequencies than at others [9]. Mechanical oscillation is the periodic repetition of mechanical vibrations. Many MEMS can be modeled using a single degree of freedom damped oscillator like the following:

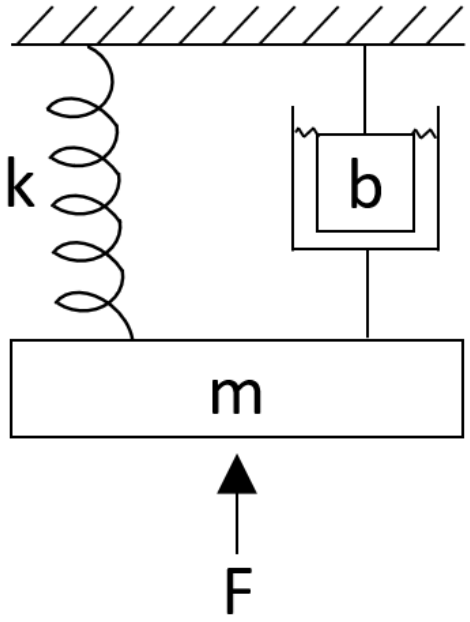

Figure 2.3: Single degree of freedom damped oscillator

The equation for motion of such a system is:

$$F(t) = mx''(t) + bx'(t) + ku(t) \quad (2.3)$$

where x is the displacement, m is the effective mass, b is the damping coefficient, k is the stiffness of the spring, and t is time. The undamped frequency of the system is:

$$\omega_0 = \sqrt{\frac{k}{m}} \tag{2.4}$$

The damping ratio (ξ) is:

$$\xi = \sqrt{\frac{b}{4km}} \tag{2.5}$$

If the system is considered to be underdamped, the complete response should be of the form:

$$x(t) = e^{-\xi(\omega_0)t}[C_1 \cos(w_d t) + C_2 \sin(w_d t)] \tag{2.6}$$

where ω_d is:

$$\omega_d = \omega_0 \sqrt{1 - \xi^2} \tag{2.7}$$

2.7 Q-Factor

The quality factor (Q) is a way to measure of energy loss in a resonator [10]. Hence, the better the Q factor, the more suited an oscillator is to its application. The Q factor drives the sharpness of the peak in a plot of response versus frequency [9]. It can be represented as:

$$Q = \frac{1}{2\xi} = \frac{\sqrt{km}}{b} \tag{2.8}$$

for a model of a single degree of freedom damped oscillator. A common Q factor definition for resonators is:

$$Q = 2\pi \frac{E_{stored}}{E_{lost}} \tag{2.9}$$

where E_{stored} is considered the stored energy in the "spring", and E_{lost} is the energy lost per steady-state vibration [9].

2.8 Temperature Compensation

One of the most effective methods for controlling the resonant frequency of a MEMS resonator (and thus the temperature) is to create an oven-control circuit. Past works done by researchers have demonstrated stability of oven-controlled MEMS resonators. Operating at an elevated temperature, this method often uses current passed through the resonator to heat the resonator [3]. Minimizing the TCF of the resonator is key in increasing its stability. If f is frequency, and T is temperature, then TCF can be defined as follows:

$$\text{TCF} = \frac{1}{f}\frac{df}{dT} \tag{2.10}$$

There are two general approaches to compensating the frequency drift due to temperature fluctuation: active temperature compensation and passive temperature compensation. Degenerately doping the silicon layer in silicon-based MEMS resonators, adding a silicon dioxide over layer, and designing the body shape of the resonator to have a low TCF are examples of passive temperature compensation [11].

Alternatively, active temperature compensation methods offer better temperature stability but often use more power. Active temperature compensation requires adjustments via external manipulation. Using active elements of a circuit for control, heating a resonator to an elevated temperature, and introducing mechanical or thermal stress are examples of active temperature compensation [11].

2.9 TPoS Resonators

The resonator to be used in this circuit is a thin-film piezoelectric-on-substrate (TPoS) resonator. This is advantageous because TPoS resonators provide a low motional impedance at

relatively high frequencies and do not need bias voltage [12]. They use a thin layer of piezoelectric material to induce resonance in the substrate, which is typically silicon [13].

2.10 Temperature Coefficient of Frequency

The temperature coefficient of frequency (TCF) describes the change in frequency as the temperature changes. The TCF for lightly doped silicon is often around -30ppm/°C and is about -50ppm/°C for most MEMS oscillators. The TCF has a bell-curve shaped; thus, the change in the TCF is minimized at the turnover temperature (where the TCF switches polarity) of the bell-curve. Keeping the resonator operating at or around this temperature will help keep the performance of device stable since the TCF is at its minimum [14].

2.11 Temperature Coefficient of Resistance

The temperature coefficient of resistance (TCR) describes the change in resistance of a material or device when its temperature is changed. A positive TCR means that the resistance increases with an increase in temperature while a negative TCR means that the resistance decreases with an increase in temperature. For some semiconductor materials, the TCF may be negative because an increase in heat increases the charge-carrier ratio and increases conductivity, decreasing the resistance.

2.12 Future Potential

MEMS are anticipated to be used in wider applications as research continues. From energy to security, MEMS have the potential to impact and improve sensing and electronic performance in countless applications. The unique properties of microdevices operating with mechanical attributes is what makes MEMS an increasing field of interest today. Some applications have, to some extent, limits on their performance that need to be reduced before MEMS can serve as a

replacement for the current industry standard counterparts. An example of this is the potential of MEMS oscillators to replace crystal oscillators, but the current TCF of the MEMS oscillators is high and needs to be minimized for it MEMS oscillators truly be a viable replace for crystal oscillators. Thus, to explore oven-control for MEMS oscillators, this project will focus on using active temperature control for a TPoS resonator.

CHAPTER 3: CIRCUIT DESIGN AND THEORY OF OPERATION

This chapter explores the design of a circuit schematic that will be used to create a printed circuit board. The objective of the circuit is to measure the voltage and current through the resistor and be able to manually tune the input voltage so that the current passed through the resonator keeps the temperature stable.

Exact values of the circuit components rely on the resistance of the resonator and the amount of current needed to be passed through it to heat the resonator to the desired temperature. The specific type of resonator used in this circuit may change the range of the input voltage wanted; thus, exact values for resistors, capacitors, and voltage references will be avoided whenever possible.

3.1 Theory of Operation

The overall function of the circuit is to aid in the temperature stabilization of a TPoS MEMS resonator. This section describes the operation of the circuit and the general purpose of its components, and the following image depicts the overall circuit schematic. Subsequent sections will detail the optimization and operational equations of each portion of the circuit.

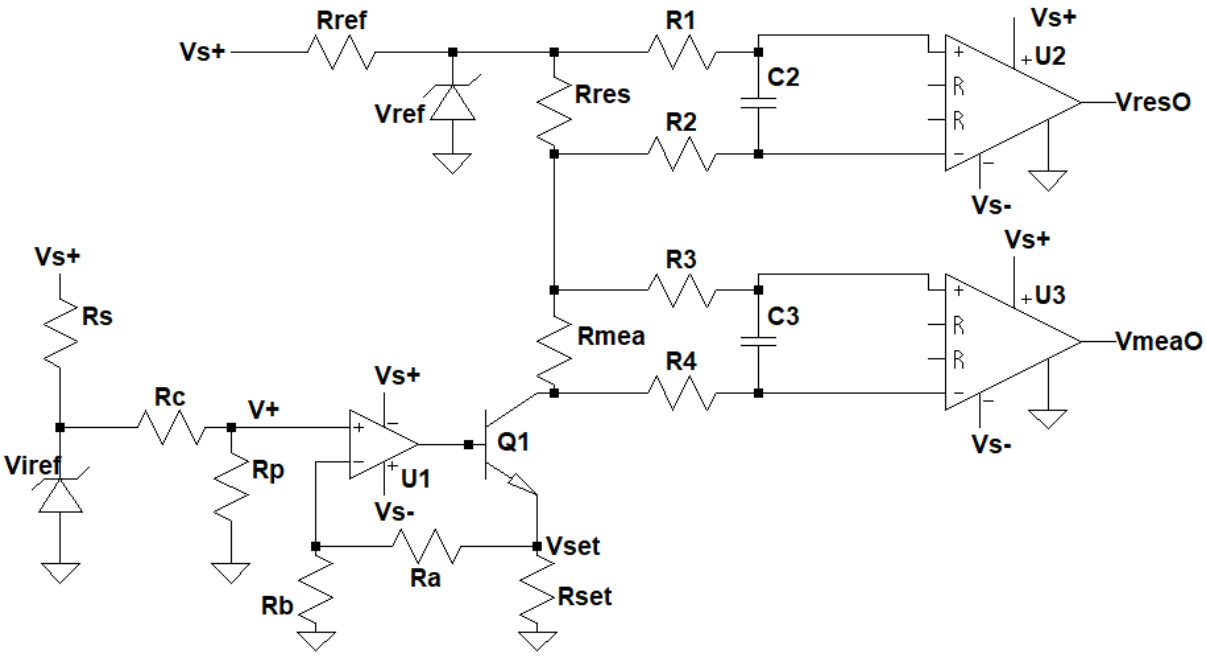

Figure 3.1: Schematic of circuit

The voltage supply powers a voltage reference (V_{iref}) that provides a stable input voltage for the circuit. Then, the potentiometer (R_p) is used to help manually tune the voltage inputted to the circuit. The resistors, R_a and R_b, are used to scale the range of the voltage input.

A voltage to current converter is used at the input to set the current passing through the resonator. The current passed through the resonator is:

$$\frac{V_{set}}{R_{set}} \approx I_{res} \tag{3.1}$$

The voltage drop across R_{res} and R_{mea} is driven by the input of a voltage reference source that provides a stable input for these components. Two instrumentation amplifiers (with first order filters to reduce noise) are used to measure the voltage across R_{res} and R_{mea}.

The output (V_{resO}) of the instrumentation amplifier measuring the voltage drop across the resonator should be equal to the voltage across the resonator, while the output (V_{meaO}) of the

instrumentation amplifier measuring the voltage drop across R_{mea} should be equal to the voltage across R_{mea}, which can result in a calculation of the current using Ohm's Law:

$$\frac{V_{meaO}}{R_{mea}} = I_{mea} = I_{res} \tag{3.2}$$

This, along with the measurement of V_{resO} can then be used to find the resistantance of the resonator using the following equation:

$$\frac{V_{resO}}{I_{mea}} = R_{res} \tag{3.3}$$

The correlation between R_{res} and the temperature, previously determined by the user, can be used to ascertain the temperature of the resonator from this calculation.

3.2 Voltage Reference for Input

A voltage reference was chosen for the input voltage since it can provide a precise input to the circuit. It is important that the chosen component has tight tolerances and provides a value that will supply the proper range of input voltage. The value for the reference resistor is chosen such that the following inequality is satisfied, where I_{qMin} and I_{qMax} are cathode current limits specified in the datasheet:

$$I_{qMin} < I_q < I_{qMax} \tag{3.4}$$

The figure below shows how a voltage reference is typically connected and is provided here to show which currents and resistors correspond to which name designations.

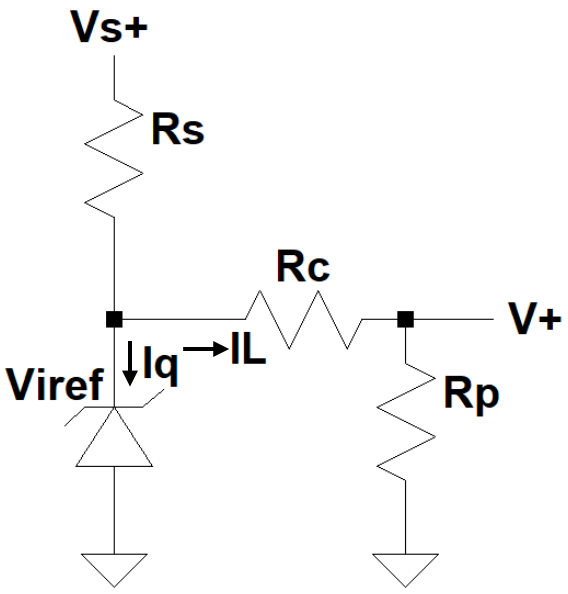

Figure 3.2: Voltage reference for input

The minimum current required at the cathode of the voltage reference for it to operate is listed in the datasheet of the voltage reference chosen, as is the maximum cathode current allowed. Sometimes, there is also a recommended value listed. The cathode current will be referred to as I_q in the following equations. R_s should be chosen to satisfy this requirement. For this configuration, the following equation must also be satisfied:

$$\frac{V_{s+} - V_{iref}}{R_s} = I_L + I_q \tag{3.5}$$

The desired value for I_q should be set to satisfy the above limits. I_L is the current value passed through R_c, and I_q is the current at the cathode of the voltage reference. Then, the voltage divider is in place to allow for control of the voltage input to the op-amp. The value that appears on the V^+ terminal is equal to the equation below, with R_p as a potentiometer for manual tuning of the input. Having the potentiometer located there also allows for total shutoff of the voltage if desired. The following equation describes the relationship between V_{iref} and V^+.

$$V^+ = \left(\frac{R_p}{R_p+R_c}\right) * V_{iref} \quad (3.6)$$

Then, the voltage at the positive terminal will be amplified to give the desired voltage range for the current passed through the resonator. This is represented by the equation shown below:

$$V_{set} = \left(\frac{R_a}{R_b} + 1\right) * V^+ \quad (3.7)$$

Thus, V_{set} is related to V_{iref} by the following equation:

$$V_{set} = \left(\frac{R_a}{R_b} + 1\right) * \left(\frac{R_p}{R_p+R_c}\right) * V_{iref} \quad (3.8)$$

3.3 Voltage to Current Converter

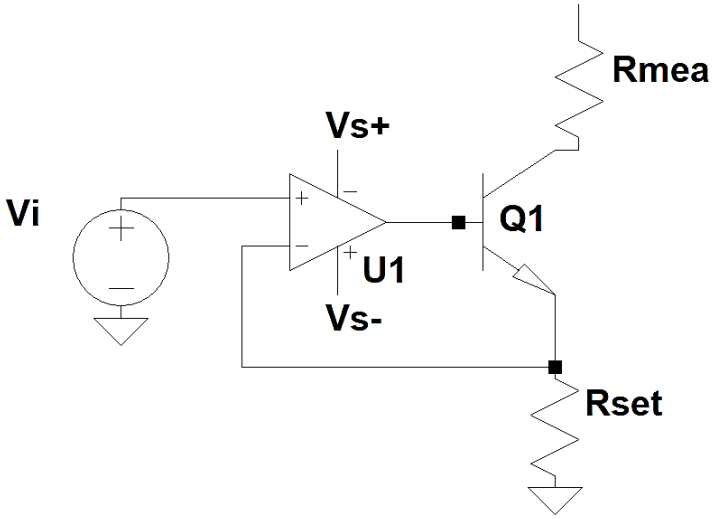

Figure 3.3: Voltage to current converter

The above figure depicts a sample voltage to current conveter. The input voltage is routed to U1 on the positive terminal and is equal to the negative terminal. Thus, the current through R_{set} is:

$$\frac{V_{in}}{R_{set}} = I_{set} \quad (3.9)$$

Then,

$$(\beta + 1)I_{mea} = \beta I_{set} = (\beta + 1)I_{res} \quad (3.10)$$

If β is sufficiently large, then

$$I_{res} \approx I_{set} \approx I_{mea} \quad (3.11)$$

The maximum input voltage can be calculated as follows:

$$V_{iM} = \frac{V_{ref} - V_t}{\left(\frac{R_a}{R_b} + 1\right)\left(\frac{R_p}{R_p + R_c}\right)} \quad (3.12)$$

An input voltage higher than V_{iM} will cause the transistor to not be in forward active mode and will negatively impact circuit performance. Thus, the voltage input should not exceed V_{iM}.

3.4 Transistor

The transistor used in this circuit is a NPN bipolar junction transistor (BJT). NPN was best suited for this circuit since it has a low turn-on voltage and a high current gain. The particular transistor chosen must have high gain (β). Using this value, the following equation can be true:

$$I_{res} \approx I_{set} \approx I_{mea} \quad (3.13)$$

3.5 First Order Filter

A first order filter is designed to attenuate noise from the voltage signals. For this application, a first order low pass filter was added to both instrumentation amplifiers. The cutoff frequency for the filter is determined by the following equation, with R and C defined as shown in Figure 3.4.

$$\frac{1}{2\pi * 2RC} = f_{cutoff} \quad (3.14)$$

The following image depicts the arrangement of the first order filter used on the instrumentation amplifiers in the circuit.

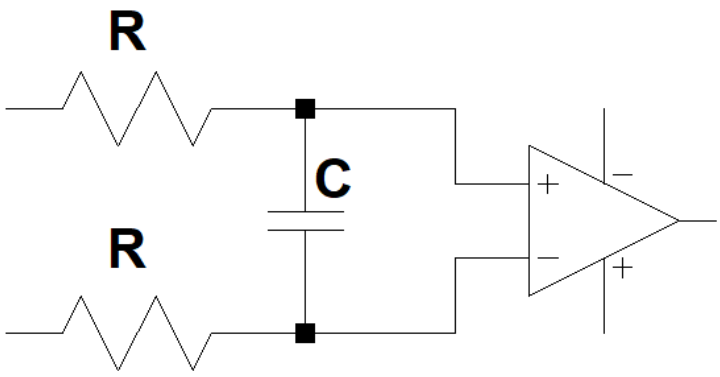

Figure 3.4: First order filter for op-amp input

3.6 Instrumentation Amplifiers

Both instrumentation amplifiers are chosen because of their low power, high precision performance. Although two devices are needed, the same component option can be used for both instrumentation amplifiers. The desired parts per billion (ppb) accuracy of the frequency of the circuit means that all of the circuit components must be very accurate. In addition to meeting performance criteria, the instrumentation amplifier must meet desired supply voltage requirements. One of the instrumentation amplifiers will be used to measure the voltage across the resonator, and the other will measure the voltage across a thermally invariant resistor to measure the current passing through the resonator. This resistor, labeled as R_{mea} in Figure 3.1, must have a very low TCR in order to be able to calculate the current through it and the resonator with high accuracy.

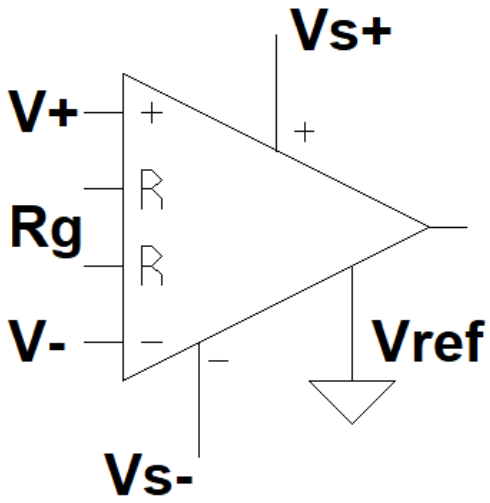

Figure 3.5: Instrumentation amplifier setup

The gain for the op-amp is set per the manufacturer datasheet by the following equation, where R_X is related to resistors inside the integrated circuit and has a predetermined value that can be found in the datasheet:

$$1 + \frac{R_X}{R_G} = \text{Gain} \tag{3.15}$$

However, for this design, across the resonator and resistor used for current measurements, a gain of 1 will be sufficient. Adding a resistor for gain on the instrumentation amplifier would not provide much advantage and would increase the thermal noise of the circuit. Thus, R_G should be left open to allow for a gain of 1.

The reference terminal is grounded because the instrumentation amplifier is used in dual-supply mode. However, if the instrumentation amplifiers were to be used in single-supply mode, the reference pin would need to have a low impedance voltage input equal to about half the supply voltage to shift the output and allow for driving of the single-supply ADC [15].

The equation of the output of each instrumentation amplifier, V_o, is described by the following equation, where G is the gain:

$$V_o = (V^+ - V^-) * G + V_{ref} \quad (3.16)$$

3.7 Voltage Reference for Powering the Resonator

The voltage reference source serves here to provide a stable input for the voltage drop across the resonator and prevents improper loading of the instrumentation amplifier. The maximum reference voltage needed can be calculated according to the following equation that is based on the maximum voltage input and its effects. V_t is the turnon voltage of the transistor, V_{setM} and V_{resM} are the maximum voltage across R_{set} and the resonator (occurs when the current I_{set} is at its highest value, referred to here as I_{setM}, and is due to V_i being at its highest value).

$$I_{setM}(R_{set} + R_{mea}) + V_{setM} + V_t = V_{refM} \quad (3.17)$$

The minimum value for the reference resistor is calculated such that the following inequality is satisfied, where I_{qMin} and I_{qMax} are cathode current limits specified in the datasheet:

$$I_{qMin} < I_q < I_{qMax} \quad (3.18)$$

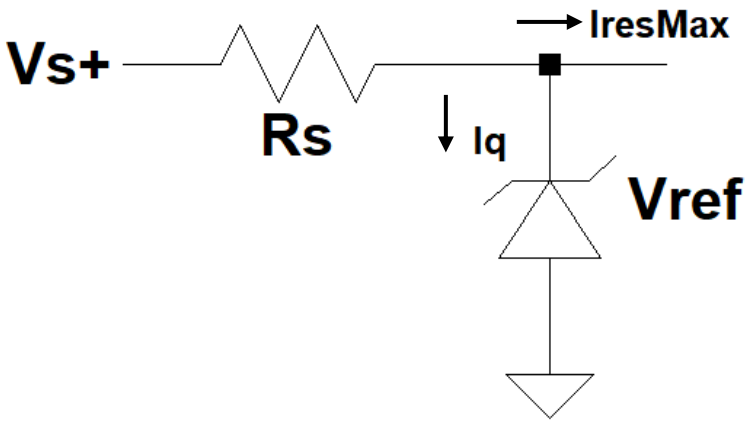

Figure 3.6: Voltage reference setup

For this configuration, the following equation must be satisfied:

$$\frac{V_{s+}-V_{ref}}{R_s} = I_{resMax} + I_q \quad (3.19)$$

I_{resMax} is the maximum current value passed through the resonator that the circuit is designed to handle, and I_q is the current at the cathode of the voltage reference. According to the datasheet, the inequality in Equation (3.20) must be satisfied in order to meet minimum operating voltage requirements while staying beneath the maximum reverse current. Thus, R_s must be chosen to satisfy this requirement. The voltage reference chosen must have a reference value which is satisfactory based on the desired I_{set} range [16].

3.8 Supply Voltages

Choosing the value for the supply voltage depends on the range of the voltage drop across R_{res}. Unless the op-amp or instrumentation amplifier supports rail-to-rail operation, it is important to set the supply voltage such that the inputs V^+ and V^- do not exceed V^+ - a and V^- + b, where 'a' and 'b' are constants listed in the datasheet such that the device will meet common-mode voltage requirements [15]. Additionally, all datasheets should be checked to ensure that the chosen supply voltage is within the specified limits for that component since all will be using the same supply voltage. Furthermore, the supply voltage much be enough to activate the voltage reference.

CHAPTER 4: PRINTED CIRCUIT BOARD DESIGN

4.1 Schematic Design

The process of the schematic design was started in Linear Technologies' software LTSpice XVII, hereafter referred to as LTSpice, and then transferred to Autodesk EAGLE.

4.1.1 Schematic in LTSpice

This program allows for modeling of the circuit from an ideal and functional standpoint before proceeding to printed circuit board design. LTSpice allows for virtual testing of the performance of the circuit to see how it would be expected to respond to external stimuli. By downloading components to the LTSpice component database, assessments of how the circuit would function could be made with precision. The following figure depicts the schematic built in LTSpice with sample component values:

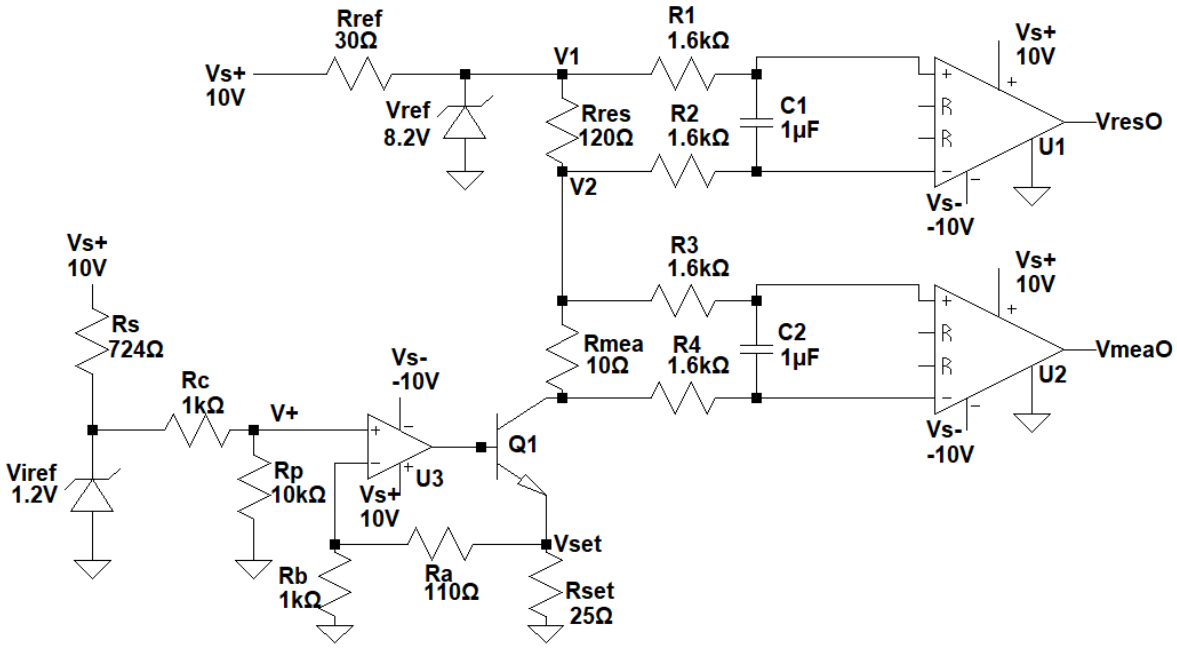

Figure 4.1: Schematic design in LTSpice with sample values

The following table details some of the relevant outputs of the simulation. These values were simulated using the component values given in the above schematic.

Table 4.1: Sample Simulated and Expected Values

Measurement	**Simulated Value**	**Expected Value**
V1	8.2V	8.2V
V2	2.1287V	2.2V
V3	1.62276V	1.7V
V+	1.12554V	1.091V
Vset	1.24936V	1.25V
VresO	6.07129V	6V
VmeaO	0.50594V	0.50V
I(Rset)	49.9746mA	50mA
I(Rmea)	50.5942mA	50mA
I(Rres)	50.5942mA	50mA

4.1.2 Schematic in EAGLE

The schematic design in EAGLE was done manually but was directly based on the design from LTSpice. During this stage of the design, the power for the circuit and the connectors had to be added to the design. Wiring the nets and naming them properly is vital to the operation of the circuit. The following image depicts the schematic design in EAGLE. The inputs and outputs can be seen in the right-hand side of the design. There are variety of test points that have been laid out for testing the assembled PCB. These are to be used for design debugging to improve future improved iterations of the PCB.

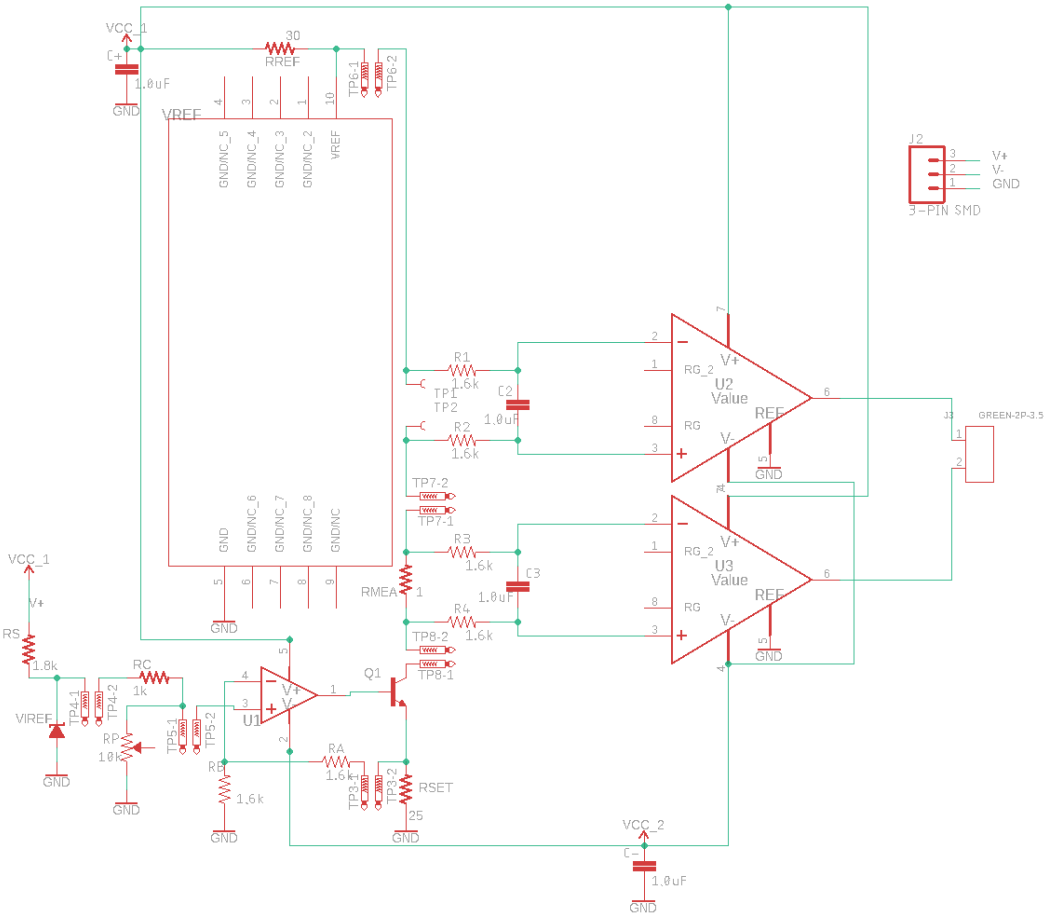

Figure 4.2: Schematic design in EAGLE

4.2 Design Considerations

Building the schematic in LTSpice, which is a suitable way to test the ideal conditions of the circuit, was a necessary first step. However, translating that into a PCB design with functional inputs and outputs requires accounting for some realistic design constraints and physical connections. The methods by which inputs and outputs are routed to the circuit will be considered in this section.

4.2.1 Voltage Input

The voltage input to the circuit is designed to be supplied using a bench supply and JST connectors on the PCB. These signals will be referred to as V_{s+} and V_{s-} throughout the following

figures. An adjustable voltage reference with a potentiometer is the input for the voltage to current converter. This provides a stable and precise input voltage.

4.2.2 Voltage Output

There will be two voltage outputs: one that is the voltage across the resonator and one that is the voltage across the 1Ω resistor. Each output will have an output to a terminal that can be plugged into a Data Acquisition Unit (DAQ) so that the voltages can be read by the user and used to calculate the resistance of the resonator using the following equation:

$$\frac{R_{mea}V_{res}}{V_{mea}} = R_{res} \tag{4.1}$$

The usage of a DAQ will allow for the data to be read and calculated in real time using National Instruments' LabView.

4.2.3 Resonator Connections

The resonator itself will be wire-bonded to two copper pads on the PCB. Thus, the PCB will be large enough that the die containing the resonator can be rested on the board to maximize bonding ease and efficiency. These copper pads will be connected directly to the circuit as shown in the schematic in Figure 4.1. In testing the circuit, a resistor can also be soldered across the terminals to examine how the circuit operates.

4.3 PCB Design

After the schematic was designed and simulated to meet specifications in LTSpice, the design was copied over to Autodesk EAGLE for design of the printed circuit board (PCB). EAGLE is a PCB design software that allows for schematic design, board layout, and routing. This software was chosen because it has a user-friendly interface and is readily available to students.

4.3.1 Ground Pours

For this PCB, ground pours were added below the top and above the bottom layers of the board. Creating a common ground in this manner has advantages since the ground pour can act as a heatsink and can help increase shielding and decrease noise. It can also allow the components to be more easily grounded because rather than having nets and traces for grounding, a simple via can connect the layer containing the component to the ground pour. For these reasons, two ground pours were added to this PCB, one on the top layer and one on the bottom layer.

4.3.2 Board Layout

The layout of components throughout the design of the PCB was an iterative process. Each time the circuit was updated, the board layout had to be modified so that the components were in optimal positions for routing and testing. While the EAGLE software automatically arranges the components, the inputs and outputs were not always in an accessible position. The auto layout places all the components of each type together, but for the sake of testing each stage of the circuit, this needed to be modified. The components were rearranged using manual placements to allow for different portions of the circuit to be grouped closer together. Since the schematic design required much updating along the way, the layout process was repeated over and over. The final board layout as created in EAGLE can be seen below. The extra space along the top of the board is for placing the die with the resonators so they can be bonded to the copper pads.

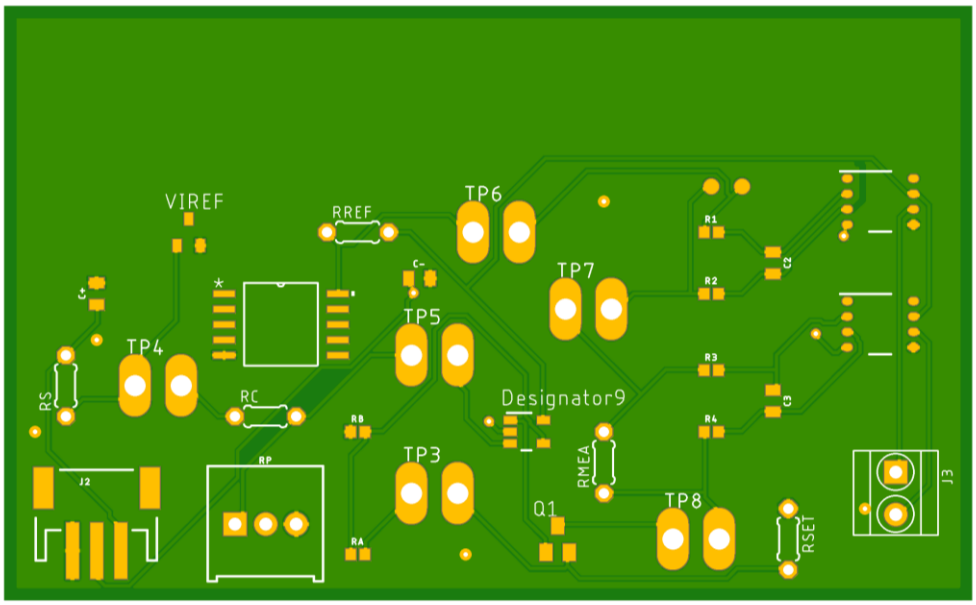

Figure 4.3: Manufacturing board layout

4.3.3 Routing

The routing for the circuit was done using the auto router. This is an option within EAGLE to have the program iterate through the most complete and efficient routing options. It operates under the parameters set by the user and can be very useful for creating initial connections on the board. When the routing is complete, the design rule check, which are also parameters set by the user but are based on the PCB manufacturer's specifications, must also be satisfied. The design rule check inspects parameters such as isolation between layers, trace clearance, distance between drill holes, pad dimensions, thermal isolation, roundness of components, mask dimensions, and more.

The following figure depicts the routed PCB design. The red and blue layers are the ground pours on the top and bottom, respectively. The traces can be seen throughout the circuit, many of them routing to vias that connect the nets to the ground pours or to other nets.

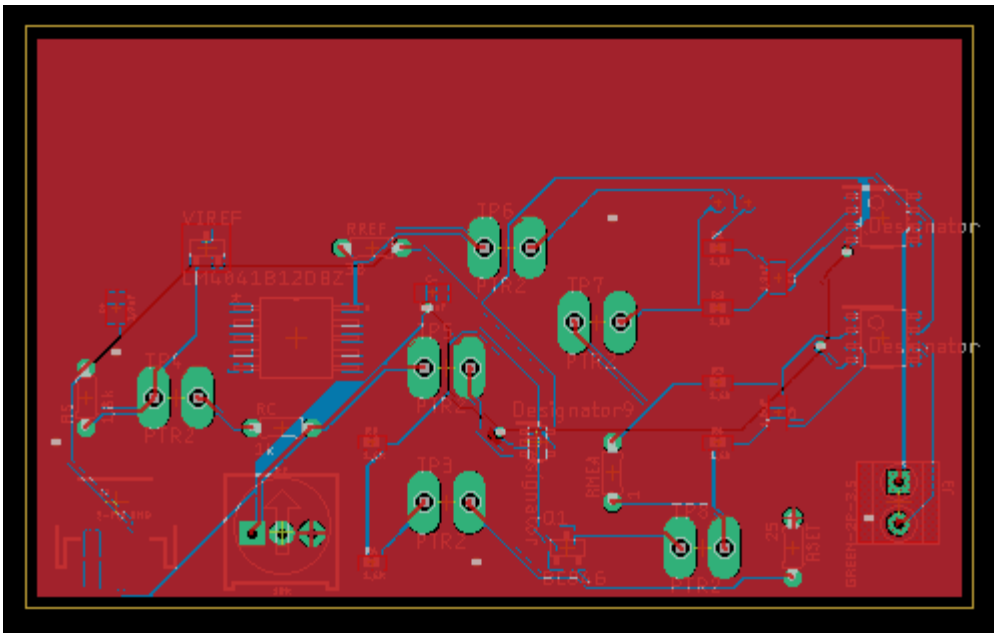

Figure 4.4: Routed PCB layout

CHAPTER 5: TEMPERATURE COMPENSATION RESULTS

5.1 Sample Temperature and Resistance Characterization

The following figure shows the process of a setup that can be used for characterizing the resistance and temperature correlation for the resonator.

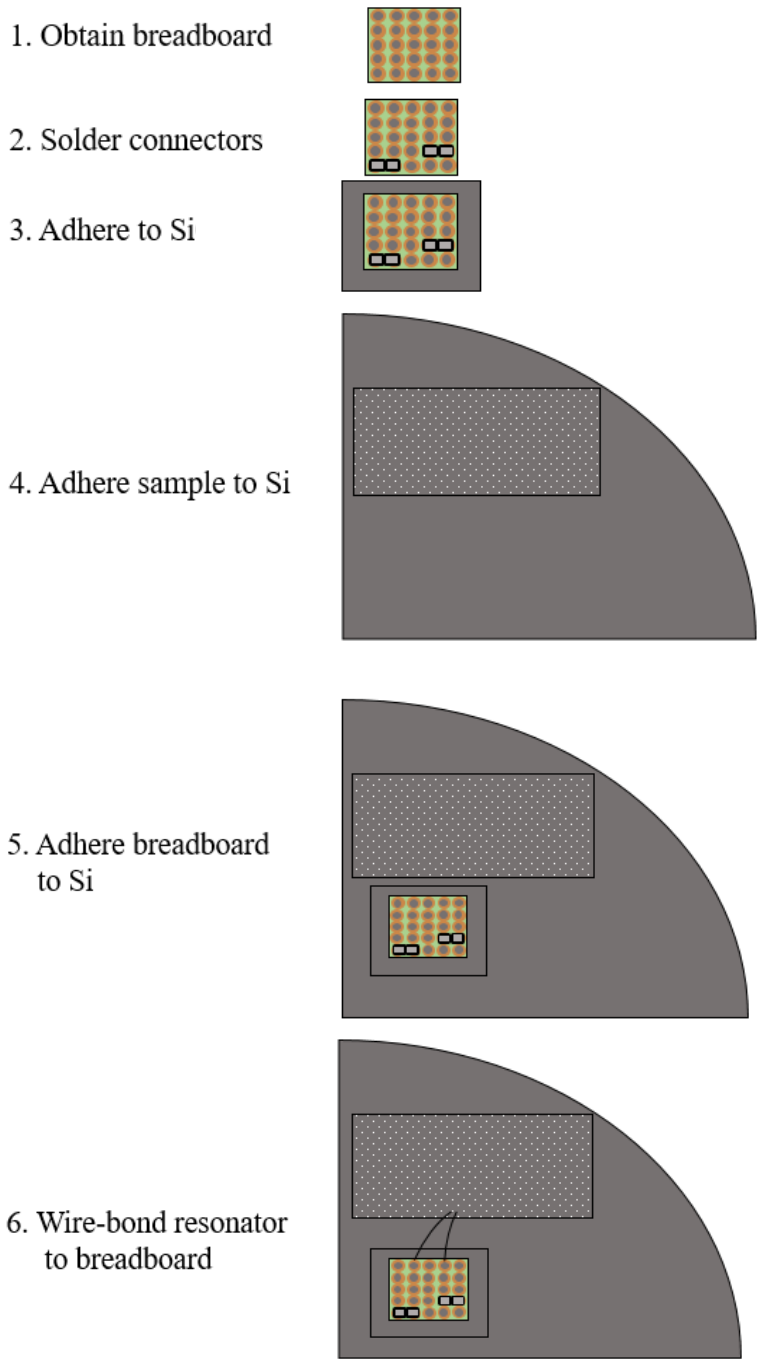

Figure 5.1: Testing setup

5.1.1 Breadboard

A small copper breadboard was used for this step. It was initially part of a larger board that was reduced in size for ease of testing.

5.1.2 Connectors

Two connector pins were soldered into the breadboard as shown in the above figure. This allowed for easier connectivity with the resonator since the pins were large enough to allow wires or clips to connect there for resistance measurements.

5.1.3 Adhere Breadboard to Si

The breadboard was then adhered to a small piece of silicon. While silicon conducts, using a layer of insulative glue for adhering this piece of silicon to another piece of silicon can prevent the two from passing unwanted current and voltage to the resonator.

5.1.4 Adhere Sample

The sample containing the resonator was adhered to a piece of silicon using thermal paste. This was chosen because the temperature of the chuck in the vacuum chamber should be close to that of the resonator. Thus, having a thermally conductive adhesive here is important.

5.1.5 Adhere Si to Si

The breadboard on silicon was then adhered to a piece of silicon near the side of the die containing the resonators. Epoxy is recommended for this adhesion since it can often withstand high temperatures. It also acts as an electrical insulator and prevents the breadboard connectors from conducting with the silicon below the resonator. Epoxy is also a strong adhesive; thus, it keeps the breadboard stable and allows for effective wire bonding.

5.1.6 Wire Bonding

For the testing described here, an ultrasonic wire bonder was used. The bonder used was a West-Bond 7400A. Optimization of bond strength and ease of bonding focused on ensuring that the substrate was secured on the stage and that the second bond was exactly 90° north of the first bond. For this wedge bonder, the aluminum wire was fed into the back of the needle at a 45° angle. Ultrasonic energy was used to melt a small bit of the wire when the user places the tip of the needle on the substrate. This created the first bond, in this case on the copper breadboard. Then, with the wire still connected to the spool, a second bond was made on the rough silicon of the resonator. The machine then severed the wire [17].

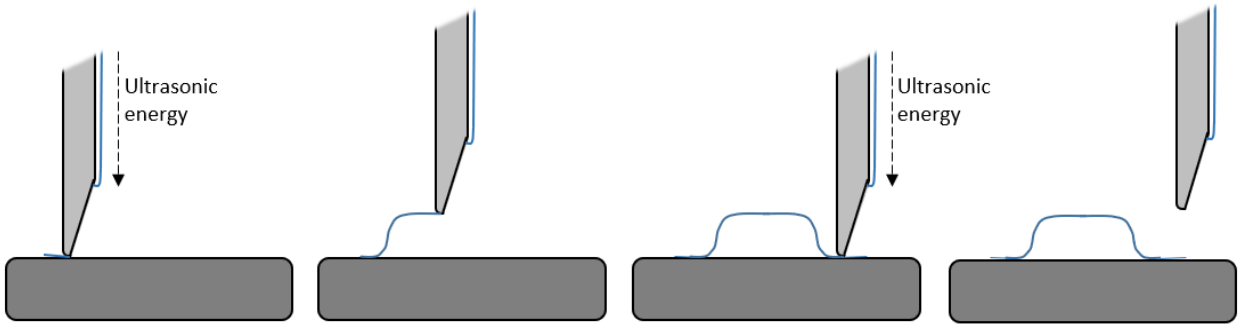

Figure 5.2: Example of wedge bond process

The time and energy of the ultrasonic pulse as well as the manual application force are what allow for user-control of the bonding process. In this case, the first bond was done at 240mJ for 300ms, and the second was done at 243mJ for 300ms.

The following image depicts the physical testing setup for the sample. The breadboard and die are on a piece of silicon, and the wire bonder needle can be seen on the right side of the image.

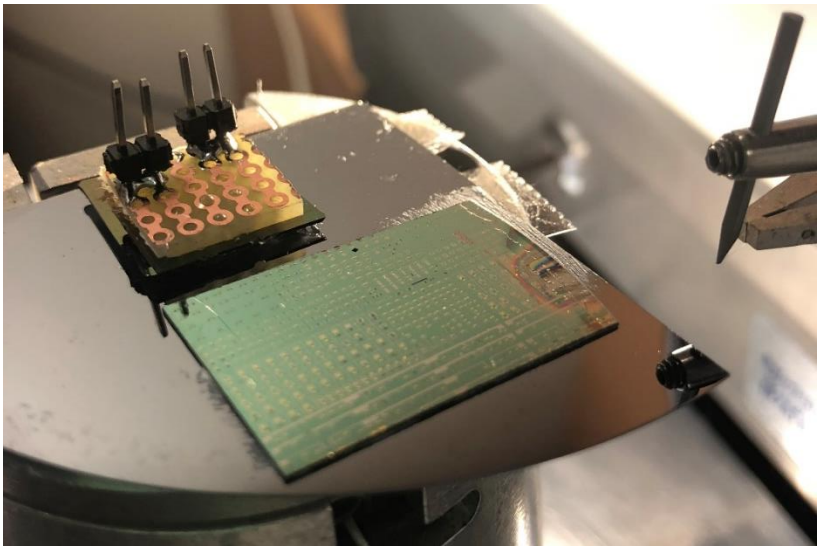

Figure 3: Actual testing setup

5.1.7 Vacuum Chamber Testing

The entire wire bonded setup detailed above was then glued into a vacuum chamber using thermal paste. The wires already inside the chamber were soldered to the connector pins on the breadboard. Those wires connected to a set of connector pins outside of the chamber. These connector pins then had leads for a multimeter soldered to them to minimize impedances from poor connections.

The sample sat on a chuck which could be heated to a certain temperature using controls outside of the chamber. Once the vacuum was activated, the pressure dropped down to approximately 1mTorr. Then, the resistance was measured at 20°C, 30°C, 40°C, and 50°C. However, when the chuck was set to 60°C, the wires bonded to the resonator would come undone.

Initially, the adherence of the sample and breadboard to the silicon and silicon dioxide was done with hot glue; however, when the full setup was placed in the vacuum chamber and heat was applied to the silicon, the wires bonded to the resonator would break. It was hypothesized that the

hot glue would soften at or above temperatures of 60°C; thus, Loctite plastic epoxy was used instead because it had an operating range up to 150°C.

This was a successful method of increasing bond strength, and the chuck could now be heated to 110°C without the bonds breaking.

CHAPTER 6: SUMMARY AND CONCLUSION

This project focuses on designing a temperature control circuit for a TPoS MEMS oscillator. The unique characteristics of the TCF of this device demonstrates the potential of the oscillator to be operated at a stable resonance frequency with ppb accuracy. Thus, this printed circuit board has been designed to be low noise and produce a precise output.

Currently, to be able to exercise ppb control, this project would need to have complete TCR data. Then, active current would need to be passed through the resonator to determine the range of current needed to heat the resonator to the temperature desired. These measurements are essential for establishing a baseline for the resistor values and voltage input range. Then, based on these values, a PCB could be ordered and used to test the resonator at a stable temperature. A DAQ would need to be programmed to read the information from the circuit and calculate the resistance.

MEMS oscillators have some beneficial characteristics compared to crystal oscillators. MEMS oscillators can be fabricated using traditional semiconductor methods and can have smaller packages. Thus, methods of minimizing their TCF, currently a disadvantage of MEMS oscillators, could be beneficial to exploring their usage.

Further research for this project could focus on utilizing digital control for controlling the current across the resonator. This would eliminate the need for a DAQ and manual control; instead, a microcontroller could be used to adaptively calculate the necessary current input to keep resonator at a constant temperature.

APPENDIX

Table 6.1: Sample Component Values for the Circuit

Name	Value
Vs+	10V
Vs-	10V
Rs	1.8kΩ
Viref	LM4041B12
Rc	1kΩ
Rp	Potentiometer
Rb	1kΩ
Ra	113Ω
Rset	25Ω
U1	OPA828
Q1	BC846
Rmea	1Ω
R3	1.6kΩ
R4	1.6kΩ
C3	1µF
U3	INA828
Rres	TPoS MEMS
R1	1.6kΩ
R2	1.6kΩ
C2	1µF
U2	INA828
Vref	LM4050
Rref	30Ω
C-	1µF
C+	1µF

REFERENCES

[1] R. Candler et al, "Frequency Stability of wafer-scale encapsulated MEMS resonators," *Digest of Technical Papers*, vol. 2, pp. 1965-1968, 2005.

[2] R. Abdolvand, *Thin-Film-Piezoelectric-On-Substrate Resonators and Narrowband Filters*, Atlanta, Georgia: Georgia Institute of Technology, 2008.

[3] Z. Wu and M. Rais-Zadeh, "A temperature-stable MEMS oscillator on an ovenized micro-platform using a PLL-based heater control system," in *28th IEEE International Conference on Micro Electro Mechanical Systems (MEMS)*, Estoril, 2015.

[4] J. Burghartz, "Microelectromechanical Systems (MEMS)," in *Guide to State-of-the-Art Electron Devices*, 1 ed., Wiley-IEEE Press, 2013, pp. 240-249.

[5] A. Ballato, "Piezoelectricity: history and new thrusts," in *IEEE Ultrasonics Symposium*, San Antonio, TX, 1996.

[6] H. Fujita, "A decade of MEMS and its future," in *IEEE The Tenth Annual International Workshop on Micro Electro Mechanical Systems. An Investigation of Micro Structures, Sensors, Actuators, Machines and Robots*, Nagoya, 1997.

[7] C. Lam, "A review of the recent development of MEMS and crystal oscillators and their impacts on the frequency control products industry," in *IEEE Ultrasonics Symposium*, Beijing, 2008.

[8] C. Liu, Foundations of MEMS, Upper Saddle River: Pearson Education, 2006, pp. 245-279.

[9] S. Heinrich and I. Dufour, "Fundamental Theory of Resonant MEMS Devices," in *Resonant MEMS: Fundamentals, Implementation, and Application*, Weinhem, Wiley-VCH, 2015, pp. 3-28.

[10] W. Pan, "Temperature Compensation of Piezo-MEMS Resonators," in *Piezoelectric MEMS Resonators*, Springer International Publishing, 2017, pp. 243-256.

[11] I. Kanno, "Piezoelectric Thin Films for MEMS Applications," in *MEMS Fundamental Technology and Applications*, Boca Raton, FL: Taylor and Francis Group, 2013, pp. 41-68.

[12] R. Abdolvand, H. Lavasani, G. Ho and F. Avazi, "Thin-film piezoelectric-on-silicon resonators for high-frequency reference oscillator applications," *IEEE Transactions on Ultrasonics, Ferroelectrics, and Frequency Control*, vol. 55, no. 12, pp. 2596-2606, December 2008.

[13] R. Abdolvand et al, "Micromachined Resonators: A Review," 2016.

[14] S. Shahraini, R. Abdolvand and H. Fatemi, "Temperature Coefficient of Frequency in Silicon-Based Cross-Sectional Quasi Lamé Mode Resonators," in *IEEE International Frequency Control Symposium*, Olympic Valley, 2018.

[15] Texas Instruments, "INA828 50-µV Offset, 7-nV/√Hz Noise, Low-Power, Precision Instrumentation Amplifier," January 2018. [Online].

[16] Texas Instruments, "LM4050-N/-Q1 Precision Micropower Shunt Voltage Reference," 2015.

[17] T. Gleditch, H. Hvims, R. Rörgren and J. Vähäkangas, "Chapter A: Wire Bonding," 2000. [Online].

[18] Texas Instruments, "OPA188 Precision, Low-Noise, Rail-to-Rail Output, 36-V, Zero-Drift," 2006.

[19] Texas Instruments, "PRECISION MICROPOWER SHUNT VOLTAGE REFERENCE," February 2006. [Online].